

Invited Review

MRI for the Diagnosis of Pulmonary Embolism

Edwin J.R. van Beek MD, PhD,^{1*} Jim M. Wild, PhD,¹ Christian Fink, MD,²
 Alan R. Moody, MD, PhD,³ Hans-Ulrich Kauczor, MD, PhD,² and
 Matthijs Oudkerk, MD, PhD⁴

Pulmonary embolism (PE) is one of the most frequently encountered clinical emergencies. The diagnosis often involves multiple diagnostic tests, which need to be carried out rapidly to assist in the safe management of the patient. Recent strides in computed tomography (CT) have made big improvements in patient management and efficiency of diagnostic imaging. This review article describes the developments in magnetic resonance (MR) techniques for the diagnosis of acute PE. Techniques include MR angiography (MRA) and thrombus imaging for direct clot visualization, perfusion MR, and combined perfusion-ventilation MR. As will be demonstrated, some of these techniques are now entering the clinical arena, and it is anticipated that MR imaging (MRI) will have an increasing role in the initial diagnosis and follow-up of patients with acute PE.

Key Words: pulmonary embolism; diagnosis; MR angiography; perfusion; ventilation; thrombus imaging
J. Magn. Reson. Imaging 2003;18:627-640.
 © 2003 Wiley-Liss, Inc.

VENOUS THROMBOEMBOLISM REMAINS ONE OF the most frequently encountered clinical dilemmas, with an estimated annual incidence of three to four suspected cases per 1000 in the general population in the Western world; proven cases of deep vein thrombosis (DVT) and pulmonary embolism (PE) of approximately 1.0 and 0.5 per 1000, respectively; and up to two million cases per year in the United States alone (1,2). Approximately 10% of patients with a proven venous thromboembolic event will not survive the first hour. In the remaining patients, a subclassification can be made of massive (e.g., life-threatening), submassive, and nonmassive PE (3). Less than 5% will suffer from massive PE. In this situation, echocardiography is generally the best (and

most speedy) approach, and treatment will consist of intravenous thrombolytics or (in rare instances) more invasive techniques such as embolectomy or interventional fragmentation (3). In the subgroup of patients with submassive PE, i.e., those with echocardiographic signs of right ventricular dysfunction, there is some evidence that more aggressive therapy may be indicated (4-6), but further studies are required. Thus, the vast majority of cases will have nonmassive PE and can undergo standard diagnostic tests.

Any diagnostic strategy has two main goals. First, the strategy must identify those patients at risk of a (potentially fatal) second event; these patients will require long-term anticoagulant therapy. Second, and of equal importance, the diagnostic approach needs to identify patients in whom anticoagulants can be safely withheld. These aims need to be assessed in the background of the risk of missed diagnosis and unnecessary treatment.

If the diagnosis is missed, there is a considerable risk of recurrence. Only one randomized trial was ever performed to assess treatment vs. placebo in patients with clinically diagnosed PE, which showed a fatal recurrence rate of 30% and a nonfatal second event in a further 30% of patients (7). Given this high incidence of secondary events, the efficacy of diagnostic strategies generally relies on follow-up of patients and assessment of mortality and morbidity from recurrent venous thromboembolism and bleeding complications.

Overall, only approximately 20% to 40% of patients who were initially suspected of PE will have their diagnosis confirmed (8-11). Thus, the group without disease is much larger than those with disease. This latter statement is particularly highlighted in view of the complications associated with anticoagulant therapy: bleeding complications in unfractionated heparin occur in approximately 3% to 4% of patients (9,12), with similar figures for low-molecular-weight heparins (13,14). Oral anticoagulant therapy is associated with a fatal bleeding risk of one per 100 treatment years and 4% to 16% nonfatal bleeding risk (15,16).

Traditionally, the diagnostic management of PE was largely concentrated around lung scintigraphy. A normal perfusion lung scan result effectively rules out PE, while a high-probability lung scan carries a positive predictive value of 90% (8,9,17). Unfortunately, 40% to 60% of lung scan results are neither normal nor high-

¹Unit of Academic Radiology, Royal Hallamshire Hospital, Sheffield, UK.

²German Cancer Research Center, Heidelberg, Germany.

³Department of Medical Imaging, Sunnybrook and Womens Health Sciences Centre, Toronto, Ontario, Canada.

⁴Department of Radiology, State University Hospital, Groningen, Netherlands.

*Address reprint requests to: E.J.R.v.B., Unit of Academic Radiology, Royal Hallamshire Hospital, Floor C, Glossop Road, Sheffield S10 2JF. E-mail: e.vanbeek@sheffield.ac.uk

Received April 18, 2003; Accepted August 21, 2003.

DOI 10.1002/jmri.10421

Published online in Wiley InterScience (www.interscience.wiley.com).

probability (the term *nondiagnostic* has been advocated).

Although conventional pulmonary angiography is (still) regarded as the reference method (18), it is invasive and carries an, albeit low, complication risk and cannot be performed in up to 20% of patients in whom the procedure is contemplated (19). Thus, developments have been aimed at establishing novel, noninvasive diagnostic modalities, which can offer a safe diagnostic outcome and will reduce the need for angiography. This includes plasma D-dimer (this is a breakdown product of fibrin) to help exclude the disease (11,20), ultrasonography of the leg veins (based on the observation that 70% to 90% of patients with PE also have demonstrable deep leg vein thrombosis) to help prove the disease (21,22), and, most prominently, the development of helical computed tomography (hCT) with CT-pulmonary angiography with or without extended CT-venography of the pelvis and leg veins (23,24).

Several diagnostic management strategies have been employed, usually combining several diagnostic modalities (10,11,20–22,25–28). These strategies have resulted in adequate diagnosis and management of patients with PE. However, they also have several disadvantages, which can be solved by the introduction of magnetic resonance imaging (MRI)-based techniques. Although MRI in the diagnosis of PE is still in its infancy, there are huge gains to be made in terms of its noninvasive nature, safe contrast agents, and (maybe most importantly) its inherent lack of ionizing radiation. This latter point has been emphasized both in general use and in pregnant patients (29,30). The most recent calculations show that with careful selection of imaging parameters, CT-pulmonary angiography can be safely performed (29,30); however, the additional use of CT-venography does carry a significant increase in radiation dose (31).

MRI of the chest has been developed relatively recently, when compared to other body areas. This was due to several difficulties, which needed to be overcome, such as the lack of protons within the chest, motion of both heart and lungs, and the susceptibility artifacts due to the interfaces between air and soft tissues. Contrast-enhanced MR angiography (MRA) enabled imaging of the large vessels. New sequences were developed to enable lung perfusion MRI, direct thrombus imaging of the entire venous system, and, more recently, the introduction of hyperpolarized 3-helium, which allows high-resolution lung ventilation imaging. The use of faster imaging sequences and the application of increased gradient-strength systems have made it feasible to image even breathless patients. This review will describe the current state of MRI in the diagnosis of venous thromboembolic disease (Table 1).

MRA

Techniques

Several methods may be employed to perform MRA, ranging from time-of-flight angiography to gadolinium-enhanced three-dimensional MRA. Time-of-flight MRA

Table 1
Magnetic Resonance Imaging Techniques That May Be Applied for Venous Thromboembolic Disease

1. MR angiography
a. Non-Gadolinium enhanced techniques
i. Time of flight MRA
ii. 3D-VUSE
b. Gadolinium-enhanced 3D MRA
i. Gadolinium
ii. Blood pool agents
2. MR direct thrombus imaging
3. MR perfusion imaging
a. Gadolinium-enhanced
i. Gadolinium direct (first pass)
ii. Blood pool agents
b. Non-Gadolinium:
i. Arterial spin labelling
ii. HASTE-type
4. MR perfusion-ventilation imaging
a. Oxygen-enhanced ventilation
b. Hyperpolarized 3-Helium ventilation
5. Imaging directed at lower extremity thrombosis
a. Direct clot imaging
b. Blood pool venography

was applied with some success for imaging of the central pulmonary arteries (32–35). However, several problems were identified, including a lack of spatial resolution, insensitivity to slow flow, motion sensitivity (both respiratory and pulsation), and field distortion artifacts. Another time-of-flight technique used variable-angle uniform signal excitation during free breathing (three-dimensional-VUSE), but this was not attempted in patients with suspected PE (36).

The introduction of higher-gradient-strength systems (>20 mT/m) and the development of short TR three-dimensional gradient echo sequences allowed the development of single breath-hold three-dimensional contrast-enhanced MRA (37–39). Depending on the patient's ability to hold his or her breath, either monophasic protocols with a high spatial resolution and scan times in the range of 20–30 seconds (39–44) or time-resolved multiphasic imaging protocols with scan times of under 10 seconds (45,46) can be applied. The use of shorter scan times allows the investigation even of severely breathless patients. While monophasic MRA protocols with a high spatial resolution achieve a diagnostic accuracy for the detection of PE comparable to helical CT (44), the diagnostic accuracy of time-resolved protocols in patients with PE remains unknown. The recent introduction of parallel MRI techniques, such as the simultaneous acquisitions of spatial harmonics (SMASH) (47) or the sensitivity encoding for fast MRI (SENSE) (48), will further improve breath-hold three-dimensional contrast-enhanced MRA (47–51). In contrast to conventional MRI, parallel MRI uses the spatial information inherent in the geometry of surface coil arrays to reduce the number of phase-encoding steps, thus leading to a faster acquisition time. In practice, parallel techniques allow a substantial improvement of the temporal and/or spatial resolution (Fig. 1). In contrast-enhanced MRA with the use of parallel ac-



Figure 1. Maximum intensity projection of parallel imaging gadolinium-enhanced MRA technique.

quisition techniques, the breath-hold duration of monophasic imaging protocols might be reduced at constant spatial resolution, or the spatial resolution of time-resolved imaging protocols might be improved at fixed breath-hold duration.

Hardware and Software Requirements

High-performance gradient systems with amplitudes in excess of 20 mT/m and slew rates over 120 mT/m/msec have enabled the development of ultrafast, short breath-hold MRA. This has seen a significant reduction of imaging time from a full breath-hold (20 seconds or more) to less than five seconds.

A prerequisite for parallel MR techniques is the utilization of numerous surface or array coils (52). A major drawback of parallel MRI is that the time saving achieved over sequential MRI is accompanied by an increase of the image noise. From experimental studies it is known that the ultimate achievable signal-to-noise ratio (SNR) for parallel MR images is closely tied to the geometry and sensitivity patterns of the coil arrays (53–55). Dedicated coil arrays developed for parallel acquisitions might overcome this limitation.

Gadolinium should be injected using a power injector and is generally followed by a saline flush (45). This generally requires a 20-G to 22-G intravenous access needle. A dose of 0.2 mmol/kg was shown as optimal, while increasing the dose did not improve image quality (56,57). Gadolinium concentration in the vessels of interest should be optimal at the time of central k-space acquisition, as this will determine the vascular signal intensity (58). Spherical and centric-elliptic phase-encoding ordering offer optimum contrast with conventional Cartesian k-space sampling (59), while interleaved spiral (51) and radial acquisitions (60) inherently oversample central k-space and are thus less sensitive to bolus passage timing. Time-resolved contrast-en-

hanced three-dimensional MRA methods (61) are the obvious extension whereby continuous three-dimensional data sets are required, thus capturing the arterial and venous phases and obviating the need for precise bolus synchronization. In sequences that require 20- to 30-second breath holds, a trial bolus may be useful to obtain optimal injection-imaging delay time (44). However, in ultrafast imaging sequences, this is no longer required in the majority of patients and a routine delay time of five seconds following the initiation of contrast injection will result in excellent-quality images in patients with suspected acute PE (62).

An alternative method of contrast involves the use of blood pool agents, several of which are under evaluation (Fig. 2). These agents circulate for a prolonged period, thus allowing prolonged imaging as well as opening the prospect of simultaneous imaging of pulmonary circulation and deep venous system of the lower extremities (63).

Images should be viewed on a workstation, which allows for imaging of source images as well as multiplanar reformatting, volume rendering, and maximum intensity projections. Thus, a true three-dimensional evaluation can take place with extended views of vessels (64).

Clinical Applications

Only limited clinical studies have evaluated the role of three-dimensional gadolinium-enhanced MRA for the diagnosis of PE in reasonable patient samples. The first study to compare MRA with pulmonary angiography obtained a sensitivity of 70% and a specificity of 100% in a group of 23 patients with PE (37). Another small



Figure 2. Normal angiogram using blood pool agent NC100150. Notice both arterial and venous systems are well depicted.

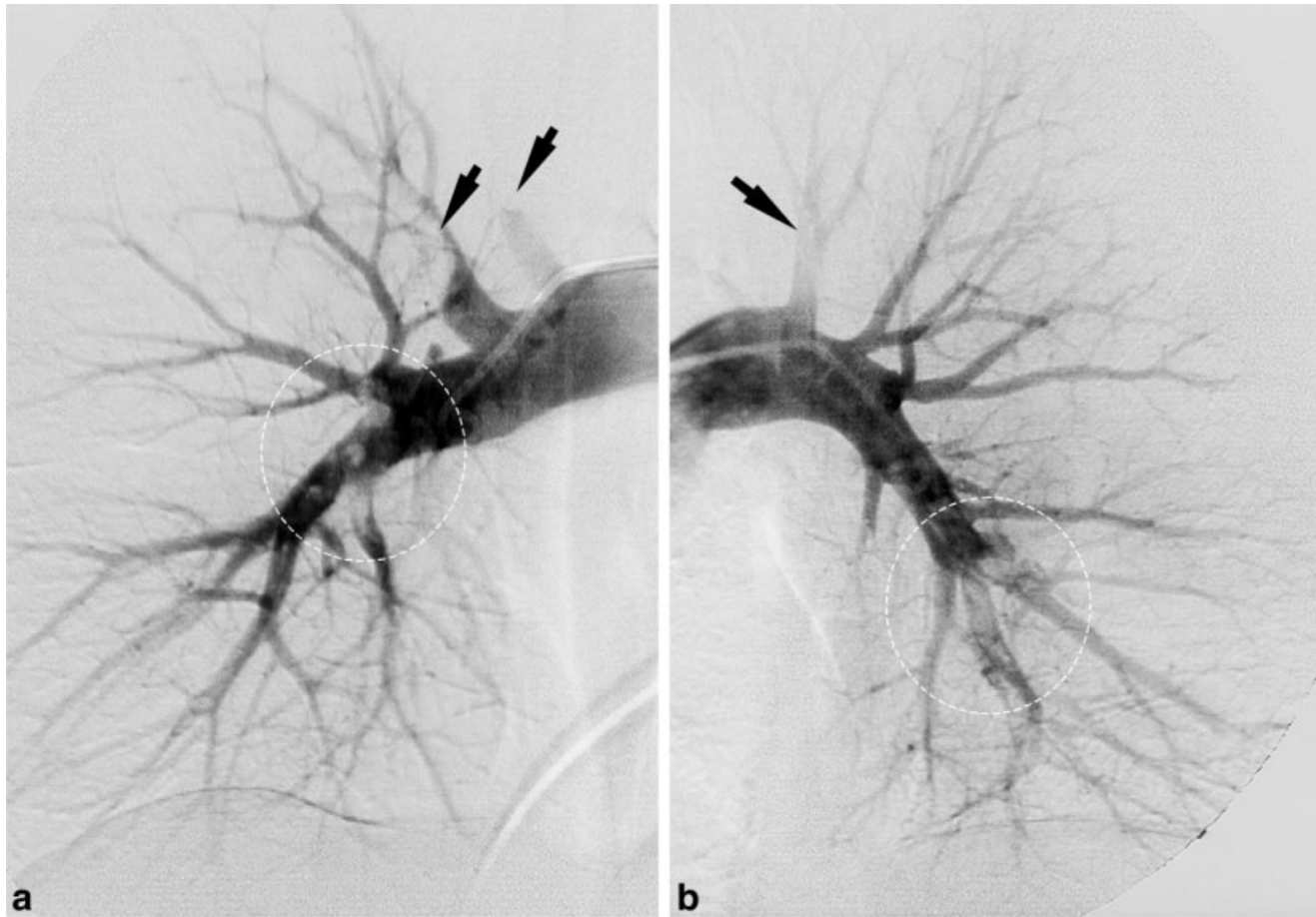


Figure 3. Conventional pulmonary angiogram of right (a) and left (b) pulmonary arteries in patient with PE. The corresponding multiplanar reformatted images of a gadolinium-enhanced three-dimensional MRA are shown for the right (c) and left (d) sides.

study evaluated three-dimensional gadolinium-enhanced MRA in 13 patients, but these patients suffered from a variety of lung disorders other than PE (40).

A pioneering study investigated the performance of a coronal gadolinium-enhanced three-dimensional time-of-flight sequence during a single breath hold in 30 patients with suspected PE (43). A total of eight patients had PEs demonstrated by angiography. The study design included independent assessment of MRA by three radiologists and the use of pulmonary angiography as a reference standard. In 10% of patients the images were of insufficient quality to be diagnostic. The interobserver correlation was good to excellent (kappa values of 0.57–0.83), while sensitivity and specificity of MRA for PE for the remaining 27 patients varied between 75% and 100%, and 95% and 100%, respectively (43). Some of the criticisms of this study were possible selection bias (no subsegmental emboli were diagnosed) and the fact that many patients with suspected PE would not be able to hold their breath for 27 seconds.

An alternative approach is to use MRA in conjunction with other diagnostic tests. Thus, using perfusion lung scintigraphy to safely exclude PE seems a cost-effective and sensible approach in terms of availability of diagnostic tests. One study took place in 36 consecutive patients with intermediate- or low-probability lung scan result and high clinical suspicion (65). Patients

underwent pulmonary angiography and MRA, and assessment of these investigations was independent. A total of 19 emboli were demonstrated in 13 patients by angiography, and MRA diagnosed 12 patients as PE (one false positive, specificity of 96%) and missed two cases (sensitivity of 85%). Both missed PEs were isolated and subsegmental in location.

A more recent study performed contrast-enhanced pulmonary three-dimensional MRA in 141 consecutive patients with an abnormal perfusion lung scintigram and compared the findings with pulmonary angiography (44). A double-contrast injection was employed with a 20-second breath hold for each lung. MRA was contraindicated in 13 patients (9%), while images were not interpretable in eight patients (6%). MRA could be performed in two patients in whom conventional pulmonary angiography was contraindicated. Thus, both MRA and pulmonary angiography were available in 118 patients (84%). Figure 3 shows a comparative study of pulmonary angiography and MRA in a patient with PE. The prevalence of PE was 30%, partially as a result of exclusion by normal scintigraphy as initial test. Images were read independently in 115 patients, and agreement was obtained in 105 cases (91%), with a kappa value of 0.75. MRA demonstrated 27 of 35 patients with confirmed emboli for an overall sensitivity of 77%. The sensitivities for isolated subsegmental, segmental, and

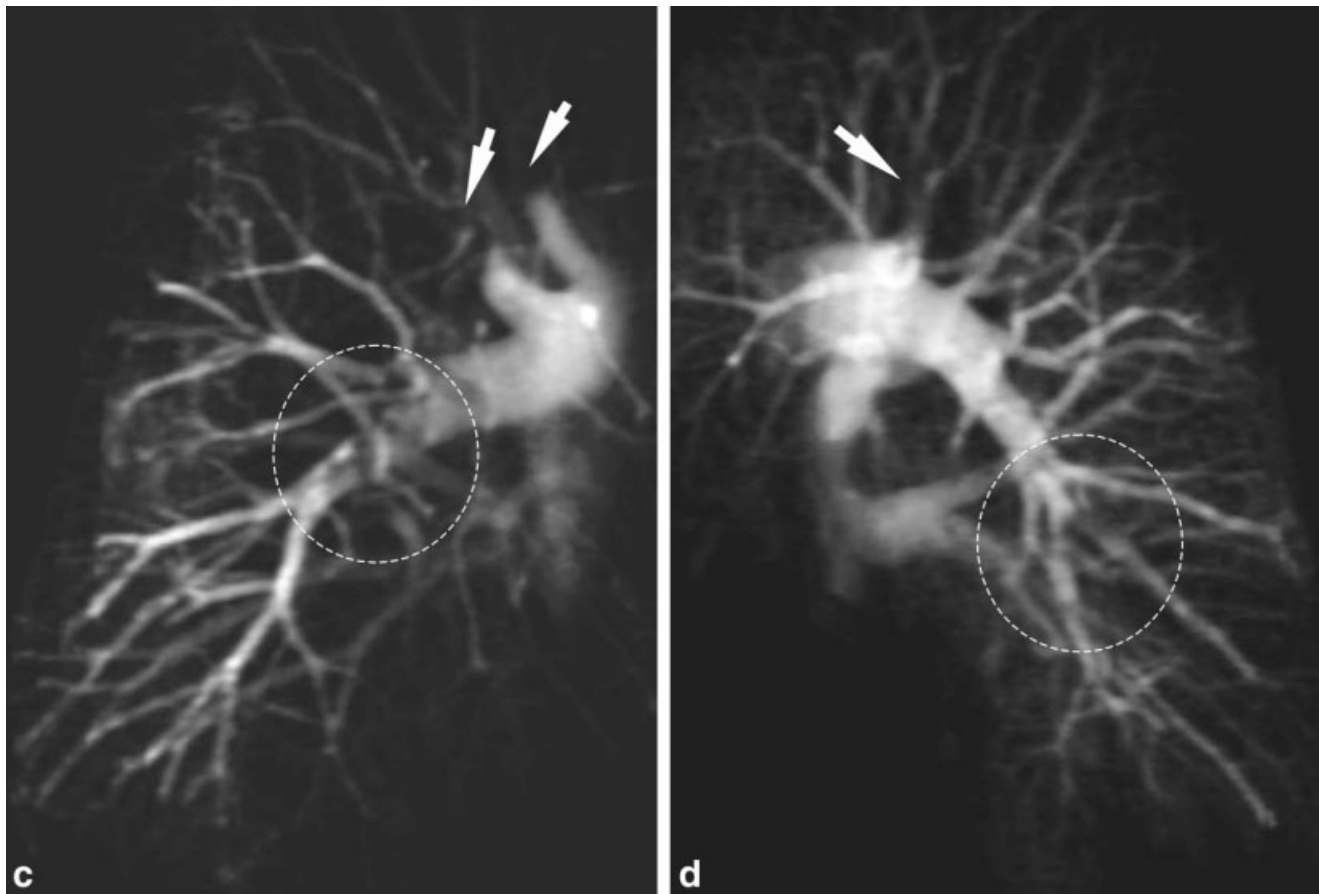


Figure 3 (Continued)

central/lobar PE were 40%, 84%, and 100%, respectively. MRA demonstrated emboli in two patients with a normal angiogram for a specificity of 98%. These latter two studies demonstrate the difficulty of diagnosing isolated subsegmental PEs, while the sensitivity for segmental or larger emboli is high (44,65). Isolated subsegmental emboli are relatively uncommon, occurring between 6% and 15% of cases (8,44,65,66). These results are comparable to the early (single-slice helical) CT data in the literature (17,23).

Most recently, the use of a short TR (1.64 msec) three-dimensional gradient echo sequence on a high-performance gradient system (1.5 T, amplitude of 40 mT/m, slew rate of 200 mT/m/msec) has resulted in a gadolinium-enhanced three-dimensional MRA sequence that can be performed in under four seconds per image data set, with five data sets acquired within a 19-second breath hold (45). The sequence has been tested in three healthy volunteers and eight dyspneic patients and demonstrated emboli in all four subsequently confirmed cases, while those without emboli were also adequately identified. A problem was that only two of the eight patients could hold their breath for 19 seconds, while all patients could hold their breath for eight seconds, during which time two data sets were acquired.

No reports using parallel acquisition techniques for three-dimensional contrast-enhanced pulmonary MRA in a large patient sample are available. Improved image quality and smaller degradation from artifacts were re-

ported in a comparative study in 20 patients using time-resolved pulmonary MRA with SENSE and electrocardiogram (ECG)-gated MRA without SENSE (50). In another study in 12 patients with known or suspected pulmonary arterial hypertension, high-resolution MRA with a 512 matrix ($0.8 \times 1.0 \times 1.5$ mm voxel size) was acquired in a 20-second breath-hold time by using partially parallel acquisition techniques (51). With this technique an excellent visualization of subsegmental vessels was possible in all cases, and the results of the MRA highly agreed with those of conventional pulmonary angiography. Despite these promising results, the diagnostic benefit over nonparallel MRA has yet to be established in a larger patient sample.

It is concluded that three-dimensional gadolinium-enhanced MRA may offer a fast, reliable test for the diagnosis of PE, but further studies will be required to confirm this. In particular, management studies will need to demonstrate the additional value of MRA, especially in terms of cost-effectiveness. The use of parallel MRI techniques might improve pulmonary MRA by improving the spatial and temporal resolution. The use of blood pool agents to image the entire venous system may be useful in the future.

MR DIRECT THROMBUS IMAGING

Direct thrombus imaging is based on the principle that blood undergoes predictable change as it clots. One

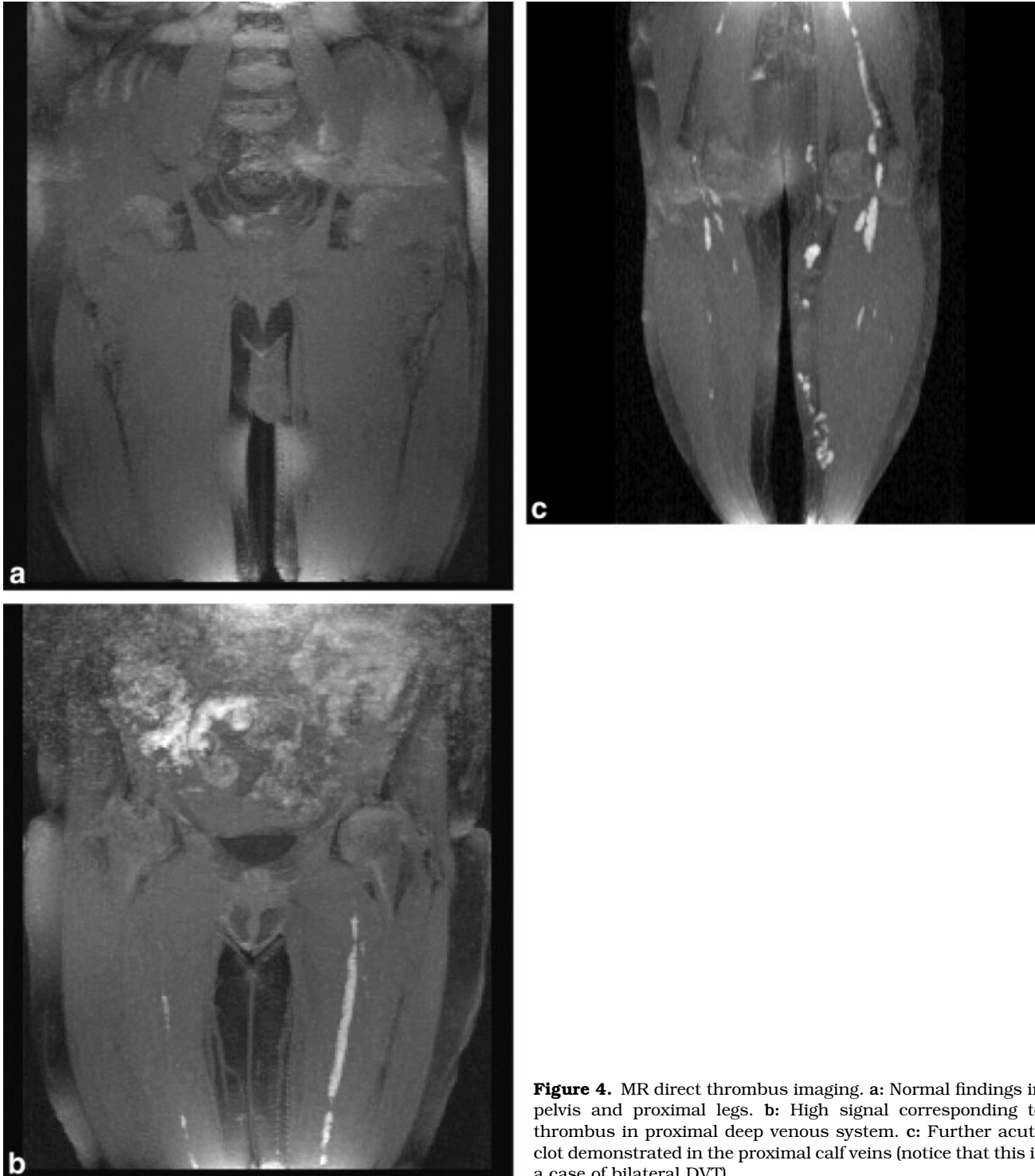


Figure 4. MR direct thrombus imaging. **a:** Normal findings in pelvis and proximal legs. **b:** High signal corresponding to thrombus in proximal deep venous system. **c:** Further acute clot demonstrated in the proximal calf veins (notice that this is a case of bilateral DVT).

intermediate product of this process is methemoglobin, which causes significant reduction in T1, and thus causes a high signal when imaged using a heavily T1-weighted sequence (67,68). This endogenous contrast can be exploited to allow the detection of subacute thrombosis directly without the need for gadolinium-based contrast agents. This technique therefore holds promise for the detection of PE and DVT (69,70). One advantage of the technique is that the presence of high signal is only seen with subacute thrombosis and there-

fore can help to differentiate between old and new clots. Initial pilot studies to detect DVT employed an MRI sequence consisting of a T1-weighted magnetization-prepared three-dimensional gradient echo sequence (71). A water-only excitation radio-frequency (RF) pulse was administered, and the effective inversion time was chosen to nullify the blood signal. Using a body coil, two imaging blocks resulted in coverage from ankle to inferior vena cava, with each block requiring $3\frac{1}{2}$ minutes acquisition time (Fig. 4).



Figure 5. MR direct thrombus imaging demonstrating a central PE in the left main pulmonary artery.

Subsequently, a study applied this technique in 101 patients with suspected DVT and compared it with conventional contrast venography (72). Although the cohort was not a consecutive group of patients, the authors prevented selection bias by including all patients with a positive venogram and randomly selecting 25% of patients who had a normal venogram result. Images were reviewed independently, and sensitivity and specificity ranged from 94% to 96% and from 90% to 92%, respectively. The interobserver agreement was formally assessed, and kappa values of greater than 0.8 were obtained. As could be expected, the diagnostic accuracy for isolated calf vein thrombosis was slightly lower than that for iliofemoral thrombosis, yielding a sensitivity range of 83% to 92%.

MR direct thrombus imaging has also been applied to the direct detection of PEs (69). This has either employed a two-dimensional or three-dimensional breath-hold acquisition. Early studies displayed the feasibility of this technique and its accuracy when applied in the clinical setting (Fig. 5). A recently concluded investigation employed MR direct thrombus imaging in the legs and chest of patients suspected of PE. Patients were randomized to the MRI study; other management strategies included 1) lung scintigraphy, followed by ultrasonography of the deep venous system of the leg if the lungscan is nondiagnostic; 2) same as strategy 1, but with pulmonary angiography as final diagnostic test if ultrasonography is normal; and 3) helical CT-pulmonary angiography (73). Outcome rather than comparison with gold standard tests was used as the end point.

The results of the study were recently presented, with 157 patients assigned to the MRI arm of the study (74). Twenty-one percent of patients did not undergo scanning. During follow-up, eight patients died (none due to thromboembolic disease) and no episodes of recurrent disease were encountered in the negative group, nor were there incidences of bleeding in the positive group.

PE was detected directly in the positive group in 19 patients and by the presence of DVT alone in 13. The outcome of the MR direct thrombus imaging management protocol was similar to that of the other management strategies. If these results can be reproduced, it would show that MR direct thrombus imaging could replace other technologies in the management of venous thromboembolic diseases and provide a comprehensive imaging technique.

PERFUSION IMAGING

Lung perfusion imaging was first developed using phase-contrast techniques, but this only allowed quantification of the left and main pulmonary arteries and was prone to errors due to flow changes and motion (75). Subsequently, the technique was developed using a variety of other sequences, which were capable of probing smaller pulmonary vessels (76–80). First, one can use gadolinium-based contrast agents and obtain perfusion information by assessment of the first-pass effect (Fig. 6). Second, one can use blood pool agents, which circulate for prolonged periods, and perform repeated data acquisitions of the pulmonary arterial circulation. Third, several noncontrast techniques may be employed invariably, using inversion recovery pulses for arterial spin labeling, followed by half-Fourier single-shot fast spin echo sequences to image the inflowing blood (81,82).

The contrast-based perfusion technique is usually combined with three-dimensional MRA, giving a dynamic enhancement of the pulmonary vascular tree similar to pulmonary angiography, which can be time-resolved to demonstrate enhancement changes during the first pass of the contrast bolus. Thus, perfusion-deficient areas can be shown, and this can aid in the visualization of PE after reconstruction of the pulmonary arterial tree. A recent publication using gadolinium-enhanced perfusion MR of the lung showed that semiquantitative evaluation of regional pulmonary perfusion may be achieved for prediction of postoperative lung function (77). This technique used a 2-mL bolus injection followed by saline flush at a rate of 3 mL/second. Three dynamic imaging sets consisting of a multislice two-dimensional inversion recovery gradient echo of six to seven seconds each were obtained during a single breath hold. The initial imaging set was obtained prior to contrast injection, while the following two were obtained seven seconds after start of bolus injection (pulmonary arterial phase) and 13 seconds after start of bolus injection (aortic phase). The technique was applied to 20 patients with potentially surgically resectable lung cancer. For comparison, pulmonary perfusion scintigraphy and pulmonary function tests were obtained, and the patients' outcomes were observed. The results showed good correlation between MR perfusion and lung scintigraphy, while MR perfusion also seemed able to predict postoperative outcome. Another study in patients following lung transplant surgery or lung reduction surgery used an adapted three-dimensional time-of-flight technique, which was adapted for imaging of both lungs during gadolinium

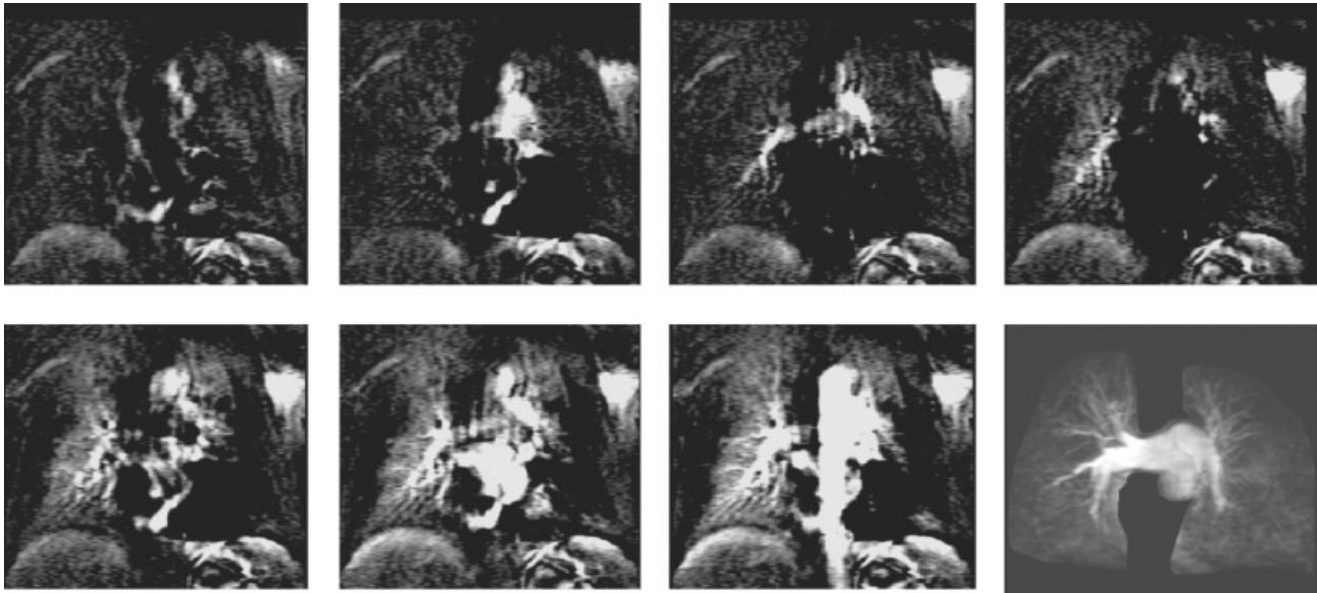


Figure 6. Left top to right bottom: Time-resolved MR subtraction angiography in a patient with chronic thromboembolic pulmonary hypertension. The first image is the subtraction image. Notice inflow and progressive perfusion with virtual absence of perfusion in the left lung. The final frame shows the corresponding gadolinium-enhanced three-dimensional MRA demonstrating absence of vasculature in the left lung.

contrast passage (three-dimensional MRA with double VUSE RF pulses) (36,83).

Several additional studies have been performed, which have added to the interpretation of perfusion MR studies. One study compared the interobserver variation of MR perfusion and scintigraphic perfusion-ventilation studies in 20 patients with PE, 11 patients with acute pneumonia, and 13 patients with chronic obstructive pulmonary disease (COPD) exacerbation (84). This study showed that the final results were closely matched, but that the interobserver variation was significantly better for MR than for lung scintigraphy.

The effects of breath holding itself has an influence on pulmonary perfusion as demonstrated in 16 patients, of which 12 were suspected to have acute PE (78). The authors compared a two-dimensional sequence with 1-second image acquisition time for 25 images with a three-dimensional sequence with five series of five seconds each. Patients were asked to hold their breath (10 patients) or breathe shallowly if they couldn't hold their breath (six patients). The findings were compared with perfusion lung scintigraphy. The results showed that in the group who could hold their breath, both sequences gave similar results, whereas in those who couldn't hold their breath, the two-dimensional sequence was more sensitive and specific for demonstration of perfusion defects. A study by the same group assessed the influence of injection rate on enhancement profiles of pulmonary parenchyma in 15 healthy volunteers (79). With increasing injection rates the peak enhancement occurred earlier, albeit that it did not affect the SNR. However, the enhancement in the aorta also occurred earlier, which could have ramifications in patients with pulmonary diseases and greater perfusion through the bronchial arterial system. It was possible to separate the pulmonary arterial perfusion from the systemic arterial perfusion using an injection rate of 3 mL/second.

Quantification of perfusion is of importance if one is to use this technique for patients' management and follow-up of treatment effects. A technique using an ultrashort TE inversion recovery two-dimensional turbo FLASH sequence was developed (85). Subsequently, this technique was shown to be successful in healthy volunteers and quantitatively validated against colored microsphere infusions in a porcine model (86).

The influence of gravity on lung perfusion is another important parameter to be considered. A study compared perfusion as obtained in six subjects in a coronal plane and six subjects in a sagittal plane to address this issue (87). The apex of the lung showed faster transit time of contrast and decreased blood volume and blood flow compared with central portions of the lung. Furthermore, the transit time was greater in gravity-dependent lung regions.

Despite these promising results of first-pass contrast-enhanced perfusion MRI of the lungs, several limitations are obvious. As the lung, unlike other organs, is characterized by a very short circulation time, perfusion MRI requires rapid imaging in order to visualize the peak enhancement of the lung parenchyma. In addition, MRI of the lung perfusion also requires a high spatial resolution and large anatomic coverage in order to reliably visualize small perfusion defects in the lung periphery, as observed in patients with PE. Although major improvements of the gradient hardware have been achieved over the last few years, previous studies dealing with MRI of lung perfusion were mostly limited to two-dimensional MRI (85,86,88). Whenever three-dimensional MRI has been attempted, the temporal and/or spatial resolution was insufficient to resolve subtle temporal changes in blood flow (76–79). Similar to contrast-enhanced MRA, it can be expected that parallel MRI will improve contrast-enhanced perfusion MRI

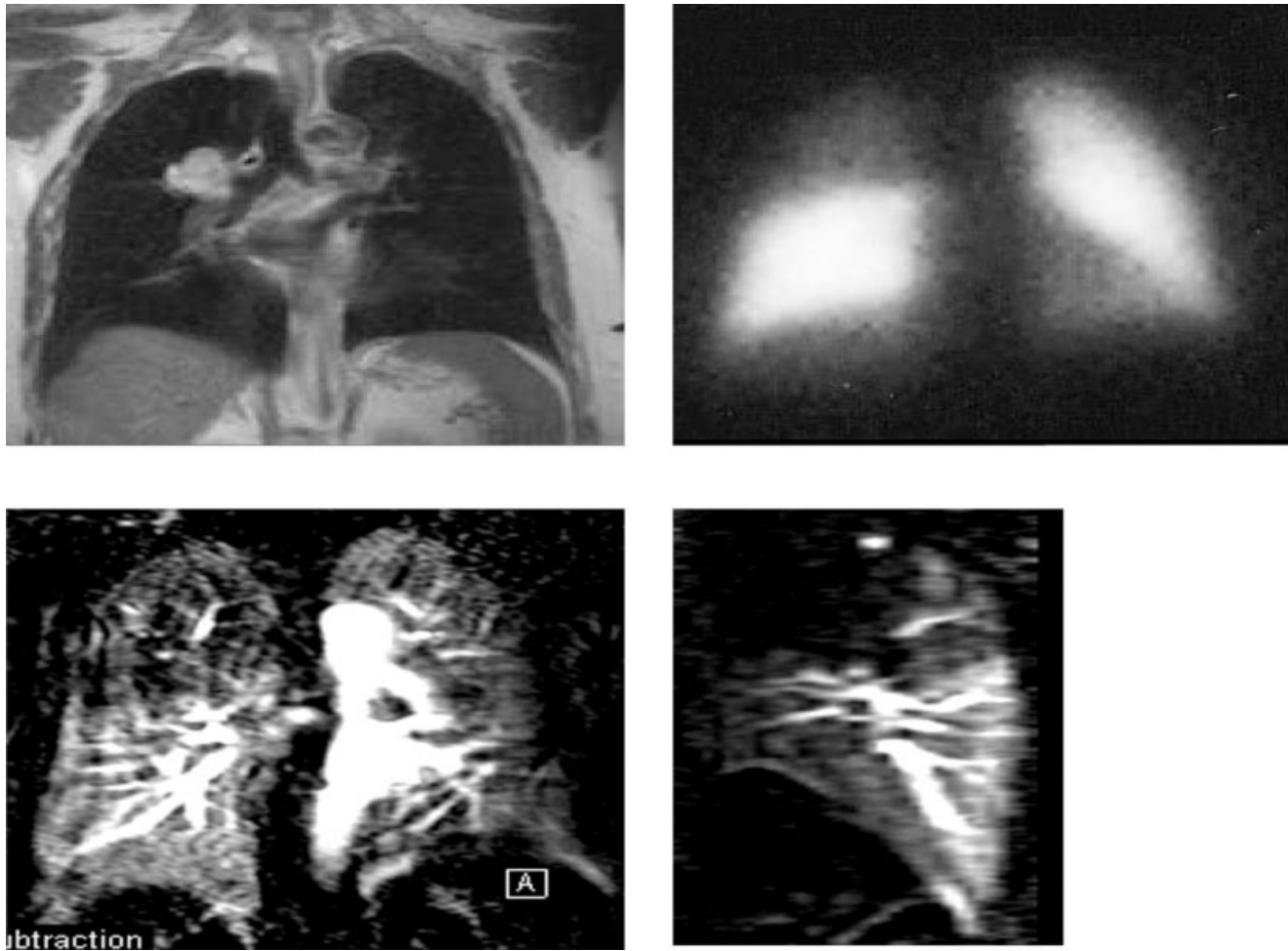


Figure 7. Three-dimensional perfusion MRI with parallel imaging techniques in a patient with a central lung cancer. Left top: Coronal HASTE. Right top: Conventional planar radionuclide perfusion scintigraphy. Bottom: Coronal and sagittal three-dimensional perfusion MR images. A perfusion defect due to the bronchus carcinoma is demonstrated.

of the lungs in terms of both spatial and temporal resolution (Fig. 7) (76–80).

Blood Pool Agent Techniques

Several types of blood pool agents have been developed, such as macromolecules that remain in the circulation or ultrasmall particles of iron oxide (USPIO). Although these agents have the advantage of prolonged imaging data acquisition, the disadvantage is that there is more overlap of arterial and venous structures. One of the first attempts in animal studies used gadolinium-DTPA-polylysine (88), and this showed good visualization down to sixth-order vessels and an increase in SNR of 120% (89). Other compounds that were tested consisted of albumin-binded gadolinium and different polymers of gadolinium, but none of these compounds were tried in human experiments (90–93).

More recently, two compounds have been studied in animals and subsequently in phase III clinical trials for cardiovascular MRA: NC100150 and MS-325 (94–97). One of these compounds was applied to perform complete venographic MR of pulmonary arteries and the

deep venous system of the legs with good results in a small number of patients (98).

Noncontrast Techniques

Arterial spin labeling techniques enable us to distinguish flowing blood from stationary tissue and thus give information on lung perfusion. Two methods have been developed for pulmonary perfusion studies, those that use precursory inversion recovery RF pulsed sequences followed by single-shot fast spin echo imaging (81,82), and those that use the concept of adiabatic fast passage with precursory pulsed field gradients to introduce continuous arterial spin labeling (99,100). The RF pulsed labeling technique has recently been used in healthy volunteers (101) and more recently in a group of nine healthy volunteers and three patients with proven PE (102). This latter study also showed the effects of the respiratory cycle, demonstrating greater SNR at end-expiration. Furthermore, a comparative study in rabbits of first-pass gadolinium MR lung perfusion and the FAIRER technique showed similar results, albeit that the gadolinium technique provided a higher SNR (103).

Another study used a single-shot half-Fourier turbo spin echo sequence (HASTE) in healthy volunteers to assess perfusion (82). This sequence applied an inversion pulse to the right ventricle and pulmonary artery, and after an inflow period, the HASTE sequence was run. More peripheral perfusion can be demonstrated by increasing the inflow time. This technique has not yet been used for the demonstration of PE. Contrast variation in pulmonary vessel intensity has also been observed in non-inversion recovery half-Fourier single-shot fast spin echo imaging (104). To minimize cardiac-dependent signal losses caused by the half-Fourier time lag between excitation and the sampling of the center of k-space, it was found that imaging should be performed after systole but before rapid filling of the ventricles. Finally, an ECG-gated fast spin echo sequence has been developed and tried in dogs with experimental pulmonary arterial and bronchial obstruction (103).

The gradient spin labeling technique was applied in eight healthy volunteers (100). This technique demonstrated the capability to distinguish between resting and postexercise blood flow changes in the pulmonary circulation. One patient with chronic obstructive pulmonary disease showed flow abnormalities.

PERFUSION-VENTILATION IMAGING

Ventilation lung MRI has become feasible using two techniques: through the use of inhaled contrast agents, such as aerosolized gadolinium and hyperpolarized noble gases, or through the use of subtraction oxygen-enhanced MRI. The advantage of ventilation imaging is not only related to direct lung function assessment, but it has also become possible to correlate perfusion and ventilation of the lung. Thus, PE is an area of particular interest, as its direct effect is a (segmental) reduction of perfusion without directly affecting ventilation (physiological responses and infarction will have a secondary effect).

Aerosolized gadolinium was combined with intravenous blood pool agents in rats (105). The model consisted of experimental PEs or large airway obstruction, and the technique was able to distinguish between them. The pulmonary parenchymal signal intensity increased by 70% due to the aerosol and a further 300% by the blood pool contrast agent. Another study used pigs and a small-particle generator, and demonstrated a signal-to-noise increase in excess of 100%, but with a time reduction of 30% (106). Finally, a study in dogs used an ultrasonic nebulizer to produce gadolinium aerosol ventilation MRI followed after 10 minutes by gadolinium-enhanced perfusion MRI (107). This study confirmed findings of those mentioned before. Initial human experiments in normal healthy volunteers were recently presented, which demonstrated homogeneous ventilation (108).

The introduction of ventilation imaging using hyperpolarized noble gases, such as 3-helium, has introduced another method to perform perfusion-ventilation imaging. One recent overview gives a good outline for technical requirements and the initial results in animals and human studies (109). Another overview fo-

cuses on the potential role within the field of lung functional imaging (110).

The feasibility of combined hyperpolarized 3-helium MRI and proton MR perfusion imaging of the lungs was initially shown in a rat model (111). A study by the same group used hyperpolarized 3-helium MRI in combination with intravenous superparamagnetic iron oxide nanoparticle perfusion MRI in a PE/airway obstruction rat model (112). Relative pulmonary blood volume maps could be superimposed on the ventilation images to demonstrate perfusion-ventilation mismatch in rats, which had PEs induced through air injection. Another study applied hyperpolarized 3-helium MR and both gadolinium-enhanced perfusion MR and gadolinium-enhanced MRA in a pig model with PE or large airway obstruction (113). It was possible to demonstrate perfusion defects with PEs, combined perfusion-ventilation defects with airway obstruction, and embolus location using MRA (Fig. 8). Very recently, a study combining hyperpolarized 3-helium MR and inversion recovery arterial spin labeling was performed in three normal volunteers, two patients following single-lung transplant for emphysema and one patient with PE (114). This showed perfusion and ventilation abnormalities in native emphysematous lungs and perfusion defects with normal corresponding ventilation in the patient with PEbolism.

Oxygen-enhanced ventilation imaging was developed around the same time as the application of hyperpolarized noble gases (115). The technique was subsequently successfully combined with gadolinium-enhanced MR perfusion imaging in a pig model of airway obstruction and/or PE (116). Oxygen-enhanced ventilation and arterial spin labeling perfusion imaging of the lungs was applied in 20 healthy volunteers, with the combination of both techniques in 10 volunteers (117). This demonstrated the feasibility of ventilation-perfusion MRI in humans. More recently, the technique was used to study 16 patients with a variety of lung diseases, including nine with PE (76). The results were encouraging, and regional perfusion deficits without ventilation abnormalities were shown in all patients with PE.

CONCLUSIONS

MRI of the chest, and in particular PE, is rapidly evolving, and the inherent advantages of noninvasiveness, nonionizing radiation requirement, the use of safer (or complete absence of) contrast agents, and the versatile sequences employed to assess various tissues in the chest render it of potential value for the future. However, it will take additional studies before one can advocate introduction in a clinical context of PE. In addition to technical considerations, the availability of MRI remains problematic in most hospitals. Thus, extension of services to include an acute disease like PE will only be possible with additional MRI time becoming available. However, as more systems are coming on-line, and with new laws on the medical use of ionizing radiation, it seems essential to develop this technology for use in the short term for those that have adequate MR resources and in the longer term for those that will have more MR capacity later. It should be emphasized that

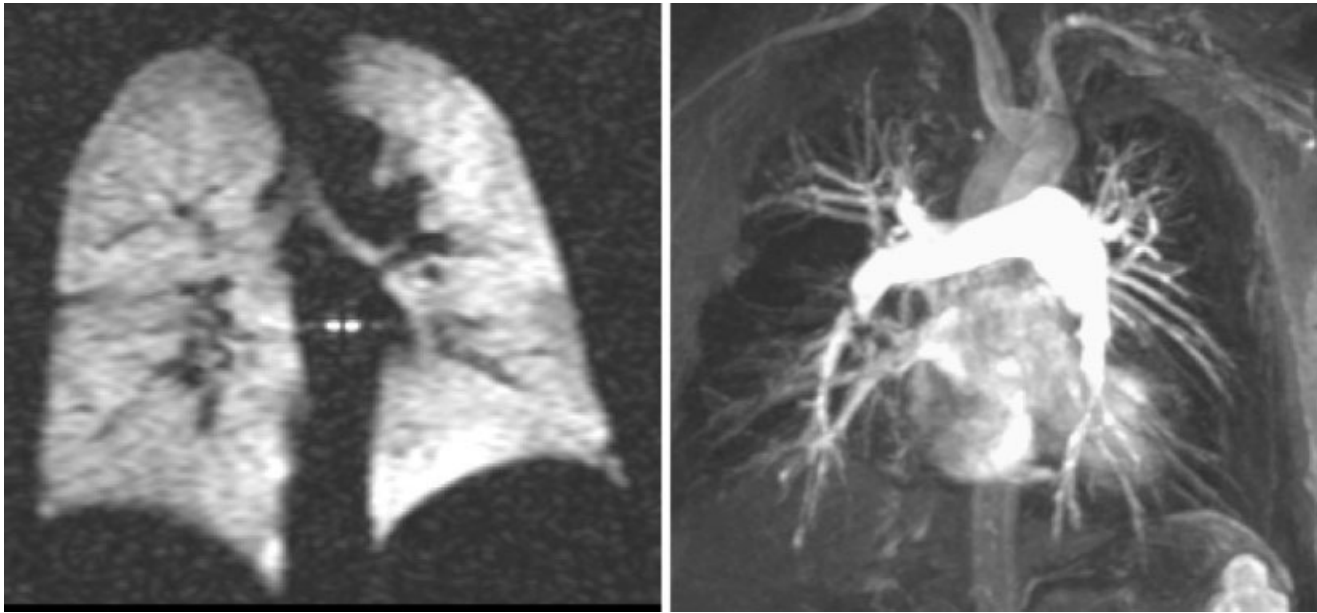


Figure 8. Hyperpolarized 3-helium MR static ventilation image (a) and corresponding gadolinium-enhanced three-dimensional MRA (b) in a patient with chronic thromboembolic disease. Notice normal ventilation in presence of extensive obstructive pulmonary vascular disease.

all work thus far has been performed on high-gradient, high-field-strength (1.5 T) systems. Additional work on low-field systems and the wider introduction of 3-T body systems is expected with interest. The use of gadolinium and hyperpolarized 3-helium could result in implementation of low-field-strength systems, while initial results on 3-T systems has shown capability of improved functional imaging within the chest. Furthermore, the introduction of blood pool agents and novel contrast techniques may change the way in which venous thromboembolic disease is imaged in the future.

REFERENCES

1. Van Beek EJR, ten Cate JW. The diagnosis of venous thromboembolism: an overview. In: Hull RD, Raskob GE, Pineo GF, editors. Venous thromboembolism: an evidence-based atlas. Armonk, NY: Futura Publishing Co.; 1996. p 93–99.
2. Hirsh J, Hoak J. Management of deep vein thrombosis and pulmonary embolism. A statement for health professionals. Council on Thrombosis (in consultation with the Council on Cardiovascular Radiology), American Heart Association. *Circulation* 1996;93:2212–2245.
3. ESC Task Force on Pulmonary Embolism. Guidelines on management of acute pulmonary embolism. *Eur Heart J* 2000;21:1301–1336.
4. Goldhaber SZ, Haire WD, Feldstein ML, et al. Alteplase versus heparin in acute pulmonary embolism: randomised trial assessing right-ventricular function and pulmonary perfusion. *Lancet* 1993;341:507–511.
5. Konstantinides S, Geibel A, Olschewski M, et al. Association between thrombolytic treatment and the prognosis of hemodynamically stable patients with major pulmonary embolism. *Circulation* 1997;96:882–888.
6. Konstantinides S, Geibel A, Heusel G, et al. Heparin plus alteplase compared with heparin alone in patients with submassive pulmonary embolism. *N Engl J Med* 2002;347:1143–1150.
7. Barritt DW, Jordan SC. Clinical features of pulmonary embolism. *Lancet*, 1961;1:729–732.
8. The PIOPED Investigators. Value of the ventilation-perfusion scan in acute pulmonary embolism. *JAMA* 1990;263:2753–2759.
9. Van Beek EJR, Kuijjer PMM, Büller HR, Brandjes DPM, PMM Bossuyt, ten Cate JW. The clinical course of patients with suspected pulmonary embolism. *Arch Intern Med* 1997;157:2593–2598.
10. Wells PS, Ginsberg JS, Anderson DR, et al. Use of a clinical model for safe management of patients with suspected pulmonary embolism. *Ann Intern Med* 1998;129:997–1005.
11. Perrier A, Desmarais S, Miron MJ, et al. Noninvasive diagnosis of venous thromboembolism. *Lancet* 1999;353:190–195.
12. Zidane M, Schram MT, Planken EW, et al. Frequency of major hemorrhage in patients treated with unfractionated intravenous heparin for deep vein thrombosis or pulmonary embolism: a study in routine clinical practice. *Arch Intern Med* 2000;160:2369–2373.
13. The Columbus investigators. Low-molecular-weight heparin in the treatment of patients with venous thromboembolism. *N Engl J Med* 1997;337:657–662.
14. Simonneau G, Sors H, Charbonnier B, et al. A comparison of low-molecular-weight heparin with unfractionated heparin for acute pulmonary embolism. *N Engl J Med* 1997;337:663–669.
15. Van der Meer FJM, Rosendaal FR, Vandenbroucke JP, Briët E. Bleeding complications in oral anticoagulant therapy. An analysis of risk factors. *Arch Intern Med* 1993;153:1557–1562.
16. Levine MN, Raskob G, Landefeld S, Hirsh J. Hemorrhagic complications of anticoagulant treatment. *Chest* 1995;108(Suppl 4):276S–290S.
17. Van Beek EJR, Brouwers EMJ, Bongaerts AH, Oudkerk M. Lung scintigraphy and helical computed tomography in the diagnosis of pulmonary embolism: a meta-analysis. *Clin Appl Thromb Hemost* 2001;7:87–92.
18. Van Beek EJR, Brouwers E, Song B, Stein PD, Oudkerk M. Clinical validity of a normal pulmonary angiogram in patients with suspected pulmonary embolism—a critical review. *Clin Radiol* 2001;56:838–842.
19. Van Beek EJR, Reekers JA, Batchelor D, Brandjes DPM, Peeters FLM, Büller HR. Feasibility, safety and clinical utility of angiography in patients with suspected pulmonary embolism and non-diagnostic lung scan findings. *Eur Radiol* 1996;6:415–419.
20. Van Beek EJR, Schenk BE, Michel BC, et al. The role of plasma D-dimer concentration in the exclusion of pulmonary embolism. *Br J Hematol* 1996;92:725–732.
21. Perrier A, Bounameaux H, Morabia A, et al. Diagnosis of pulmonary embolism by a decision analysis-based strategy including clinical probability, D-dimer levels, and ultrasonography: a management study. *Arch Intern Med* 1996;156:531–536.

22. Turkstra F, Kuijter PMM, van Beek EJR, Brandjes DPM, Büller HR, ten Cate JW. Value of compression ultrasonography for the detection of deep venous thrombosis in patients suspected of having pulmonary embolism. *Ann Intern Med* 1997;126:775-781.
23. Ghaye B, Remy J, Remy-Jardin M. Non-traumatic thoracic emergencies: CT diagnosis of acute pulmonary embolism: the first 10 years. *Eur Radiol* 2002;12:1886-1905.
24. Ghaye B, Dondelinger RF. Non-traumatic thoracic emergencies: CT venography in an integrated diagnostic strategy of acute pulmonary embolism and venous thrombosis. *Eur Radiol* 2002;12:1906-1921.
25. Oudkerk M, Van Beek EJR, Van Putten WLJ, Büller HR. Cost-effectiveness analysis of various strategies in the diagnostic management of pulmonary embolism. *Arch Intern Med* 1993;153:947-954.
26. Ginsberg JS. Management of venous thromboembolism. *N Engl J Med* 1998;335:1816-1823.
27. Goodman LR, Lipchik RJ, Kuzo RS, Liu Y, McAuliffe RL, O'Brien DJ. Subsequent pulmonary embolism: risk after a negative helical CT pulmonary angiogram—prospective comparison with scintigraphy. *Radiology* 2000;215:535-542.
28. Tillie-Leblond I, Mastora I, Radenne F, et al. Risk of pulmonary embolism after a negative spiral CT angiogram in patients with pulmonary disease: 1-year clinical follow-up study. *Radiology* 2002;223:461-467.
29. Prokop M. Radiation dose. In: Prokop M, Galanski M, editors. *Spiral and multislice CT of the body*. New York: Thieme Medical Publishers; 2002. p 131-160.
30. Winer Muram HT, Boone JM, Brown HL, Jennings SG, Mabie WC, Lombardo GT. Pulmonary embolism in pregnant patients: fetal radiation dose with helical CT. *Radiology* 2002;224:487-492.
31. Rademaker J, Grieshaber V, Hidajat N, Oestmann JW, Felix R. Combined CT pulmonary angiography and venography for diagnosis of pulmonary embolism and deep vein thrombosis: radiation dose. *J Thorac Imaging* 2001;16:297-299.
32. MacFall JR, Sostman HD, Foo TKF. Thick-section, single breath-hold magnetic resonance pulmonary angiography. *Invest Radiol* 1992;27:318-322.
33. Kauczor HU, Gamroth AH, Tuengerthal S, et al. MR angiography: clinical applications in thoracic surgery. *Eur Radiol* 1992;2:214-222.
34. Wielopolski P, Haacke E, Adler L. Evaluation of the pulmonary vasculature with three-dimensional magnetic resonance imaging techniques. *MAGMA* 1993;1:21-34.
35. Schiebler ML, Holland GA, Hatabu H, et al. Suspected pulmonary embolism: prospective evaluation with pulmonary MR angiography. *Radiology* 1993;189:125-131.
36. Friedli JL, Paschal CB, Loyd JE, Halliburton SS. Quantitative 3D VUSE pulmonary MRA. *Magn Reson Imaging* 1999;17:363-370.
37. Loubeyre P, Revel D, Douek P, et al. Dynamic contrast enhanced MR angiography of pulmonary embolism: comparison with pulmonary angiography. *AJR Am J Roentgenol* 1994;162:1035-1039.
38. Leung D, McKinnon G, Davis C, Pfammatter T, Krestin G, Debatin J. Breath-hold, contrast-enhanced, three-dimensional MR angiography. *Radiologie* 1996;201:569-571.
39. Steiner P, McKinnon GC, Romanowski B, Goehde SC, Hany T, Debatin JF. Contrast-enhanced, ultrafast 3D pulmonary MR angiography in a single breath hold: initial assessment of imaging performance. *J Magn Reson Imaging* 1997;7:177-182.
40. Isoda H, Ushimi T, Masui T, et al. Clinical evaluation of pulmonary 3D time-of-flight MRA with breath-holding using contrast media. *J Comput Assist Tomogr* 1995;19:911-919.
41. Wielopolski P, Hicks S, Obdeijn AIM, Oudkerk M. PE detection using contrast-enhanced breathhold 3D magnetic resonance angiography. Preliminary experience. In: *Proceedings of the 4th Annual Meeting of ISMRM*, New York, 1996. p 705.
42. Leung DA, Debatin JF. Three-dimensional contrast-enhanced magnetic resonance angiography of the thoracic vasculature. *Eur Radiol* 1997;7:981-989.
43. Meaney JFM, Weg JG, Chenevert TL, et al. Diagnosis of pulmonary embolism with magnetic resonance angiography. *N Engl J Med* 1997;336:1422-1427.
44. Oudkerk M, Van Beek EJR, Wielopolski P, et al. Comparison of contrast-enhanced MRA and DSA for the diagnosis of pulmonary embolism: results of a prospective study in 141 consecutive patients with an abnormal perfusion lung scan. *Lancet* 2002;359:1643-1647.
45. Goyen M, Laub G, Ladd ME, et al. Dynamic 3D MR angiography of the pulmonary arteries in under four seconds. *J Magn Reson Imaging* 2001;13:372-377.
46. Schoenberg SO, Essig M, Bock M, Hawighorst H, Sharafuddin M, Knopp MV. Comprehensive MR evaluation of renovascular disease in five breath holds. *J Magn Reson Imaging* 1999;10:347-356.
47. Sodickson DK, Manning WJ. Simultaneous acquisition of spatial harmonics (SMASH): fast imaging with radiofrequency coil arrays. *Magn Reson Med* 1997;38:591-603.
48. Pruessmann KP, Weiger M, Scheidegger MB, Boesiger P. SENSE: sensitivity encoding for fast MRI. *Magn Reson Med* 1999;42:952-962.
49. Weiger M, Pruessmann KP, Kassner A, et al. Contrast-enhanced 3D MRA using SENSE. *J Magn Reson Imaging* 2000;12:671-677.
50. Fujii M, Ohno Y, Kawamitsu H, et al. Multiphase 3D contrast-enhanced MRA of the lung using SENSE. In: *Proceedings of the 10th Annual Meeting of ISMRM*, Honolulu, 2002. p 1780.
51. Nikolaou K, Schoenberg SO, Nittka M, et al. Magnetic resonance imaging in the diagnosis of pulmonary arterial hypertension: high resolution angiography and fast perfusion imaging using intelligent parallel acquisition techniques (iPAT). *Radiology* 2002;225(P):473.
52. Nitz WR. Fast and ultrafast non-echo-planar MR imaging techniques. *Eur Radiol* 2002;12:2866-2882.
53. Hunold P, Maderwald S, Ladd ME, et al. Parallel acquisition techniques for cardiac cine MRA: comparison of image quality. In: *Proceedings of the 10th Annual Meeting of ISMRM*, Honolulu, 2002. p 1664.
54. Sodickson DK, McKenzie CA, Ohliger MA, Yeh EN, Price MD. Recent advances in image reconstruction, coil sensitivity calibration, and coil array design for SMASH and generalized parallel MRI. *MAGMA* 2002;13:158-163.
55. Madore B, Pelc NJ. SMASH and SENSE: experimental and numerical comparisons. *Magn Reson Med* 2001;45:1103-1111.
56. Boos M, Lentschig M, Scheffler K, Bongartz GM, Steinbrich W. Contrast enhanced magnetic resonance angiography of peripheral vessels. Different contrast agent applications and sequence strategies: a review. *Invest Radiol* 1998;33:538-546.
57. Hany TF, Schmidt M, Hilfiker PR, Steiner P, Bachmann U, Debatin JF. Optimization of contrast dosage for gadolinium enhanced 3D MRA of the pulmonary and renal arteries. *Magn Reson Imaging* 1998;16:901-906.
58. Maki JH, Prince MR, Londy FJ, Chenevert TL. The effects of time varying intravascular signal intensity and k space acquisition order on three dimensional MR angiography image quality. *J Magn Reson Imaging* 1996;6:642-651.
59. Wilman AH, Riederer SJ. Performance of an elliptical centric view order for signal enhancement and motion artifact suppression in breath-hold three-dimensional gradient echo imaging. *Magn Reson Med* 1997;38:793-802.
60. Peters DC, Korosec FR, Grist TM, et al. Undersampled projection reconstruction applied to MR angiography. *Magn Reson Med* 2000;43:91-101.
61. Korosec FR, Frayne R, Grist TM, Mistretta CA. Time-resolved contrast-enhanced 3D MR angiography. *Magn Reson Med* 1996;36:345-351.
62. Kauczor HU. Contrast-enhanced magnetic resonance angiography of the pulmonary vasculature. A review. *Invest Radiol* 1998;33:606-617.
63. Hoffmann U, Loewe C, Bernhard C, et al. MRA of the lower extremities in patients with pulmonary embolism using a blood pool contrast agent: initial experience. *J Magn Reson Imaging* 2002;15:429-437.
64. Davis CP, Hany TF, Wildermuth S, Schmidt M, Debatin JF. Post-processing techniques for gadolinium enhanced three-dimensional MR angiography. *Radiographics* 1997;17:1061-1077.
65. Gupta A, Frazer CK, Ferguson JM, et al. Acute pulmonary embolism: diagnosis with MR angiography. *Radiology* 1999;210:353-359.
66. Oser RF, Zuckermann DA, Gutierrez FR, Brink JA. Anatomic distribution of pulmonary emboli at pulmonary angiography: implications for cross-sectional imaging. *Radiology* 1996;199:31-35.
67. Cohen MD, McGuire W, Cory DA, Smith JA. MR appearance of blood and blood products: an in vitro study. *AJR Am J Roentgenol* 1986;146:1293-1297.

68. Sostman D, Pope CF, Smith GJW, Carbo P, Core JC. Proton relaxation in experimental clots varies with the method of preparation. *Invest Radiol* 1987;22:509–512.
69. Moody AR, Liddicoat A, Krarup K. Magnetic resonance pulmonary angiography and direct imaging of embolus for the detection of pulmonary emboli. *Invest Radiol* 1997;32:431–440.
70. Moody AR, Pollock JG, O'Connor AR, Bagnall M. Lower-limb deep venous thrombosis direct MR imaging of the thrombus. *Radiology* 1998;209:349–355.
71. Moody AR. Direct imaging of deep vein thrombosis with magnetic resonance imaging [Letter]. *Lancet* 1997;350:1073.
72. Fraser DGW, Moody AR, Morgan PS, Martel AL, Davidson I. Diagnosis of lower-limb deep venous thrombosis: a prospective blinded study of magnetic resonance direct thrombus imaging. *Ann Intern Med* 2002;136:89–98.
73. Crossley I, Moorby S, Delay S, Macdonald I, Moody A. A randomised trial comparing four methods of investigating patients with suspected pulmonary embolism: the pulmonary embolism diagnosis at Queens (PDQ) trial [Abstract]. *Radiology* 2001;221(P):213.
74. Moody AR, Crossley I, Moorby S, Delay G. Magnetic resonance direct thrombus imaging (MRDTI) as a first line investigation for pulmonary embolism—the PDQ trial. In: Proceedings of the 11th Annual Meeting of ISMRM, Toronto, Canada, 2003.
75. Silverman JM, Julien PJ, Herfkens RJ, Pelc NJ. Quantitative differential pulmonary perfusion: MR imaging versus radionuclide lung scanning. *Radiology* 1993;189:699–701.
76. Nakagawa R, Sakuma H, Murashima S, Ishida N, Matsumura K, Takeda K. Pulmonary ventilation-perfusion MR imaging in clinical patients. *J Magn Reson Imaging* 2001;14:419–424.
77. Iwasawa T, Saito K, Ogawa N, Ishiwa N, Kurihara H. Prediction of postoperative pulmonary function using perfusion magnetic resonance imaging of the lung. *J Magn Reson Imaging* 2002;16:685–692.
78. Matsuoka S, Uchiyama K, Shima H, et al. Detectability of pulmonary perfusion defect and influence of breath holding on contrast-enhanced thick-slice 2D and on 3D MR pulmonary perfusion images. *J Magn Reson Imaging* 2001;14:580–585.
79. Matsuoka S, Uchiyama K, Shima H, et al. Effect of the rate of gadolinium injection on magnetic resonance pulmonary perfusion imaging. *J Magn Reson Imaging* 2002;15:108–113.
80. Fink C, Bock M, Puderbach M, Schmähl A, Delorme S. Partially parallel three-dimensional magnetic resonance imaging for the assessment of lung perfusion—initial results. *Invest Radiol* 2003;38:482–488.
81. Mai VM, Chen Q, Bankier AA, et al. Imaging pulmonary blood flow and perfusion using phase-sensitive selective inversion recovery. *Magn Reson Med* 2000;43:793–795.
82. Hatabu H, Tadamura E, Prasad PV, Chen Q, Buxton R, Edelman RR. Noninvasive pulmonary perfusion imaging by STAR-HASTE sequence. *Magn Reson Med* 2000;44:808–812.
83. Halliburton SS, Paschal CB, Rothpletz JD, Loyd JE. Estimation and visualization of regional and global pulmonary perfusion with 3D magnetic resonance angiography. *J Magn Reson Imaging* 2001;14:734–740.
84. Amundsen T, Torheim G, Kvistad KA, et al. Perfusion abnormalities in pulmonary embolism studied with perfusion MRI and ventilation-perfusion scintigraphy: an intra-modality and inter-modality agreement study. *J Magn Reson Imaging* 2002;15:386–394.
85. Hatabu H, Gaa J, Kim D, Li W, Prasad PV, Edelman RR. Pulmonary perfusion: qualitative assessment with dynamic contrast-enhanced MRI using ultra-short TE and inversion recovery turbo FLASH. *Magn Reson Med* 1996;36:503–508.
86. Hatabu H, Tadamura E, Levin DL, et al. Quantitative assessment of pulmonary perfusion with dynamic contrast-enhanced MRI. *Magn Reson Med* 1999;42:1033–1038.
87. Levin DL, Chen Q, Zhang M, Edelman RR, Hatabu H. Evaluation of regional pulmonary perfusion using ultrafast magnetic resonance imaging. *Magn Reson Med* 2001;46:166–171.
88. Berthezene Y, Vexler V, Price DC, et al. Magnetic resonance imaging detection of an experimental pulmonary perfusion deficit using a macromolecular contrast agent: polylysine-gadolinium-DTPA₄₀. *Invest Radiol* 1992;27:346–351.
89. Böck J, Pison U, Kaufmann F, Felix R. Gd-DTPA-polylysine-enhanced pulmonary time-of-flight MR angiography. *J Magn Reson Imaging* 1994;4:473–476.
90. Zheng J, Carr J, Harris K, et al. Three-dimensional MR pulmonary perfusion imaging and angiography with an injection of a new blood pool contrast agent B-22956/1. *J Magn Reson Imaging* 2001;14:425–432.
91. Abolmaali ND, Hietschold V, Appold S, Ebert W, Vogl TJ. Gadomer-17-enhanced 3D navigator-echo MR angiography of the pulmonary arteries in pigs. *Eur Radiol* 2002;12:692–697.
92. Li KCP, Pelc LR, Napel SA, et al. MRI of pulmonary emboli using Gd-DTPA-polyethylene glycol polymer enhanced 3D fast gradient echo technique in a canine model. *Magn Reson Imaging* 1997;15:543–550.
93. Dong Q, Hurst DR, Weinmann HJ, Chenevert TL, Londy FL, Prince MR. Magnetic resonance angiography with gadomer-17. An animal study original investigation. *Invest Radiol* 1998;33:699–708.
94. Ahlstrom KH, Johansson LO, Rodenburg JB, Ragnarsson AS, Akson P, Borseth A. Pulmonary MR angiography with ultrasmall superparamagnetic iron oxide particles as a blood pool agent and a navigator echo for respiratory gating: a pilot study. *Radiology* 1999;211:865–869.
95. Grist TM, Korosec FC, Eite S, et al. Steady-state and dynamic MR angiography with MR-325: initial experience in humans. *Radiology* 1998;207:539–544.
96. Taylor AM, Panting JR, Keegan J, et al. Safety and preliminary findings with the intravascular contrast agent NC100150 injection for MR coronary angiography. *J Magn Reson Imaging* 1999;9:220–227.
97. Bremerich J, Roberts TP, Wendland MF, et al. Three-dimensional MR imaging of pulmonary vessels and parenchyma with NC 100150 injection (Clariscan). *J Magn Reson Imaging* 2000;11:622–628.
98. Hoffmann U, Loewe C, Bernhard C, et al. MRA of the lower extremities in patients with pulmonary embolism using a blood pool contrast agent: initial experience. *J Magn Reson Imaging* 2002;15:429–437.
99. Mai VM, Berr SS. MR perfusion imaging of pulmonary parenchyma using pulsed arterial spin labelling techniques: FAIRER and FAIR. *J Magn Reson Imaging* 1999;9:483–387.
100. Roberts DA, Gefter WB, Hirsch JA, et al. Pulmonary perfusion: respiratory-triggered three-dimensional MR imaging with arterial spin tagging—preliminary results in healthy volunteers. *Radiology* 1999;212:890–895.
101. Mai VM, Chen Q, Bankier AA, et al. Effect of lung inflation on arterial spin labelling signal in MR perfusion imaging of human lung. *J Magn Reson Imaging* 2001;13:954–959.
102. Keilholz SD, Mai VM, Berr SS, Fujiwara N, Hagspiel KD. Comparison of first-pass Gd-DOTA and FAIRER MR perfusion imaging in a rabbit model of pulmonary embolism. *J Magn Reson Imaging* 2002;16:168–171.
103. Suga K, Ogasawara N, Okada M, Tsukuda T, Matsunaga N, Miyazaki M. Lung perfusion impairments in pulmonary embolic and airway obstruction with noncontrast MR imaging. *J Appl Physiol* 2002;92:2439–2451.
104. Knight-Scott J, Keilholz-George SD, Mai VM, Christopher JM. Temporal dynamics of blood flow effects in half-Fourier fast spin echo (1)H magnetic resonance imaging of the human lungs. *J Magn Reson Imaging* 2001;14:411–418.
105. Berthezene Y, Vexler V, Clément O, Mühler A, Moseley ME, Brasch RC. Contrast-enhanced MR imaging of the lung: assessments of ventilation and perfusion. *Radiology* 1992;183:667–672.
106. Haage P, Adam G, Karaagac S, et al. Mechanical delivery of aerosolised gadolinium-DTPA for pulmonary ventilation assessment in MR imaging. *Invest Radiol* 2001;36:240–243.
107. Suga K, Ogasawara N, Okada M, Matsunaga N, Arai M. Regional lung functional impairment in acute airway obstruction and pulmonary embolic dog models assessed with gadolinium-based aerosol ventilation and perfusion magnetic resonance imaging. *Invest Radiol* 2002;37:281–291.
108. Haage P, Kraagac S, Spuentrup E, Pfeffer J, Guenther RW. Magnet resonance visualization of lung ventilation using aerosolised gadopentetate dimeglumine: first clinical experience [Abstract]. *Radiology* 2002;225(P):348.
109. Möller HE, Chen XJ, Saam B, et al. MRI of the lungs using hyperpolarized noble gases. *Magn Reson Med* 2002;47:1029–1051.
110. Kauczor H-U, Chen XJ, van Beek EJR, Schreiber WG. Pulmonary ventilation imaged by magnetic resonance: at the doorstep of clinical application. *Eur Respir J* 2001;17:1–16.

111. Cremillieux Y, Berthezène Y, Humblot H, et al. A combined ^1H perfusion/ ^3He ventilation NMR study in rat lungs. *Magn Reson Med* 1999;41:645–658.
112. Viallon M, Berthezène Y, Décorps M, et al. Laser-polarized ^3He as a probe for dynamic regional measurements of lung perfusion and ventilation using magnetic resonance imaging. *Magn Reson Med* 2000;44:1–4.
113. Zheng J, Leawoods JC, Nolte M, et al. Combined MR proton lung perfusion/angiography and helium ventilation: potential for detecting pulmonary emboli and ventilation defects. *Magn Reson Med* 2002;47:433–438.
114. Lipson DA, Roberts DA, Hansen-Flaschen J, et al. Pulmonary ventilation and perfusion scanning using hyperpolarized helium-3 MRI and arterial spin tagging in healthy normal subjects and in pulmonary embolism and orthotopic lung transplant patients. *Magn Reson Med* 2002;47:1073–1076.
115. Edelman RR, Hatabu H, Radamura E, Li W, Prasad PV. Noninvasive assessment of regional ventilation in the human lung using oxygen-enhanced magnetic resonance imaging. *Nat Med* 1996;2:1236–1239.
116. Chen Q, Levin DL, Kim D, et al. Pulmonary disorders: ventilation-perfusion MR imaging with animal models. *Radiology* 1999;213:871–879.
117. Mai VM, Bankier AA, Prasad PV, et al. MR ventilation-perfusion imaging of human lung using oxygen-enhanced and arterial spin labelling techniques. *J Magn Reson Imaging* 2001;14:574–579.